**Geomechanics and Engineering**, *Vol. 16, No. 2 (2018) 195-204*
DOI: https://doi.org/10.12989/gae.2018.16.2.195


# The rock fragmentation mechanism and plastic energy dissipation analysis of rock indentation

Xiaohua Zhu[*1] and Weiji Liu[**1,2]

[1]*School of Mechatronic Engineering, Southwest Petroleum University, Chengdu 610500, China*
[2]*Postdoctoral Research Station for Oil and Gas Engineering, Southwest Petroleum University, Chengdu, Sichuan, 610500, China*

*(Received August 14, 2017, Revised March 9, 2018, Accepted June 12, 2018)*

**Abstract.** Based on theories of rock mechanics, rock fragmentation, mechanics of elasto-plasticity, and energy dissipation etc., a method is presented for evaluating the rock fragmentation efficiency by using plastic energy dissipation ratio as an index. Using the presented method, the fragmentation efficiency of rocks with different strengths (corresponding to soft, intermediately hard and hard ones) under indentation is analyzed and compared. The theoretical and numerical simulation analyses are then combined with experimental results to systematically reveal the fragmentation mechanism of rocks under indentation of indenter. The results indicate that the fragmentation efficiency of rocks is higher when the plastic energy dissipation ratio is lower, and hence the drilling efficiency is higher. For the rocks with higher hardness and brittleness, the plastic energy dissipation ratio of the rocks at crush is lower. For rocks with lower hardness and brittleness (such as sandstone), most of the work done by the indenter to the rocks is transferred to the elastic and plastic energy of the rocks. However, most of such work is transferred to the elastic energy when the hardness and the brittleness of the rocks are higher. The plastic deformation is small and little energy is dissipated for brittle crush, and the elastic energy is mainly transferred to the kinetic energy of the rock fragment. The plastic energy ratio is proved to produce more accurate assessment on the fragmentation efficiency of rocks, and the presented method can provide a theoretical basis for the optimization of drill bit and selection of well drilling as well as for the selection of the rock fragmentation ways.

**Keywords:** rock indentation; rock fragmentation mechanism; ductile-brittle failure; plastic energy dissipation ratio; rock fragmentation efficiency

## 1. Introduction

In the worldwide, the low drilling efficiency is the key factor influencing the oil & gas reservoir exploration cost. How to improve the drilling efficiency and to reduce the drilling cost is a long-term difficult problem met in oil & gas drilling engineering. To solve this problem, systematic research studies on rock fragmentation mechanism are necessary to be carried out. Many investigations on the mechanism of rock fragmentation were reported in the literature. Souissi *et al.* (2015) carried out experimental tests of three kinds of rocks (granite, limestone and sandstone) under single and double indentations, and they analyzed the physical (energy dissipation and strain) and microstructural properties (radius of crushed region and crack mode) of the rocks in the indentation process. The nondestructive techniques of acoustic emission and electronic speckle pattern interferometry have used to monitor rock damage process, the initiation and propagation of crack and the size of damage zone (Zhang *et al.* 2012, 2013a, b, Chen and Labuz 2006, 2009, Mo *et al.* 2012, Yin *et al.* 2014). The stress distribution beneath the indenter together with the crack initiation and propagation were analyzed based on Griffith theory (Lawn and Wilshaw 1975, Lawn and Swain 1975, Lawn and Evans 1977). Studies were reported on the relationship between the indentation force and the lateral and radial cracks crack during the indentation process of the indenter into the brittle material, and the equations for determining the critical lengths of the radial and the lateral cracks were derived (Marshall 1984, Swain and Hagan 1976). Some researchers (Johnson 1970, 1987, Alehossein 2000) analyzed the indentation process of indenter to the rocks by using cavity expansion models, and others (Han *et al.* 2006, Huang *et al.* 1998, Carpinteri *et al.* 2004, 2005, Paluszny and Zimmerman 2014) also analyzes the indentation process by using finite element method. Some other methods, such as displacement discontinuity method (DDM) (Tan *et al.* 1998), software RFPA2D (Wang *et al.* 2011) and software R-T2D (Liu *et al.* 2002) were also used to analyze the crack propagation in the indentation process. Discrete element method (DEM) was used to investigate the failure process of rocks under indentation of wedge-shaped tool (Huang and Detournay 2013, Zhu *et al.* 2016).

The above studies aim to understand the mechanism of rock fragmentation during the indentation process, and such results play a significant role in improving the drilling efficiency. Meanwhile, different rock fragmentation techniques were also developed by researchers to improve

*Corresponding author, Professor
E-mail: zxhth113@163.com
**Corresponding author, Ph.D.
E-mail: lwjzq1111@163.com



ISSN: 2005-307X (Print), 2092-6219 (Online)

the fragmentation efficiency and drilling efficiency of rocks, such as PDC and Roller Cone impact method (Melamed *et al.* 2000, Tao 1998), torsional impact cutting method (Gillis *et al.* 2004, Zhu *et al.* 2014), and the mixed form of above two methods, particle impact method (Kuang *et al.* 2012, Ren *et al.* 2011), laser breaking method (Sinha and Gour 2006, Xu *et al.* 2003), water-jet breaking method (Xu 2004, Ni *et al.* 2004, Kolle 2000), thermal breaking method (Augustine 2009, Wilkinson and Tester 1993), ultrasonic vibration breaking method (Oothoudt 1999, Sherrit *et al.* 2000) and so on. Regarding on the breaking efficiency and drilling efficiency of rocks, Teale (1965) suggested to evaluate the drilling efficiency by using a ratio of MSE to the uni-axial compressive strength of rocks. Thereafter, many other researchers (Zhou *et al.* 2012, 2014, Chen *et al.* 2015, Rajabov *et al.* 2012, Martinez *et al.* 2013, Mendoza 2013) paid more attention to the investigation on MSE, and MSE has been used for a long time as an index to identify the fragmentation efficiency of drilling tool for rocks. However, MSE is a macroscopic method, and it cannot reveal the energy diffusion in the rock fragmentation in a micro-scale, which causes this method not to provide more accurate assessment on the efficiency of rock fragmentation. This study then presents a new concept of plastic energy dissipation ratio, and this ratio is used to evaluate the rock fragmentation efficiency.

It is well known that there are two failure modes of rocks under indentation, namely ductile and brittle failures. The drill bit may fail prematurely due to the high MSE and low fragmentation efficiency of rocks under ductile failure, and hence brittle failure is expected in the rock fragmentation. In the ductile failure of rocks, the work done by the indenter to the rocks is mainly dissipated in the elastic deformation, plastic deformation and plastic flowing. However, such work is mainly dissipated in the elastic and plastic deformations and the crack propagation when brittle failure occurs in the rocks. It is then found that the plastic deformation is unavoidable in the process of rock fragmentation, and the fragmentation efficiency of the rocks is much lower when more plastic energy is dissipated. It is a significant problem to study how to reduce the energy dissipation of plastic deformation in the rocks during the rock fragmentation. As mentioned in the above, MSE cannot assess the fragmentation efficiency of rocks in a micro-scale although it has been used as an index for a long time to produce such evaluation. To overcome such deficiency, plastic energy dissipation ratio is presented in this study to analyze the fragmentation efficiency of rocks under different conditions. This method provides a new basis for the optimization of drill bit, drilling parameters and rock fragmentation ways to improve the drilling efficiency and reduce drilling cost eventually.

## 2. Cavity expansion model

The cavity expansion model provides an approach to study the stress state of rocks before crack initiation during the indentation process. The cavity expansion model can be simply summarized as a problem of volume equilibrium (Huang 1999, Detournay 1995). For brevity, a

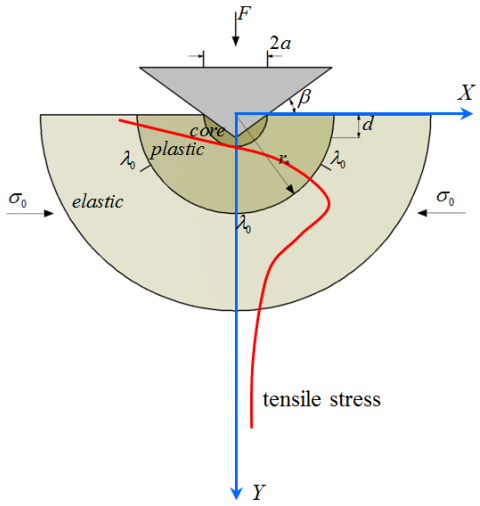


Fig. 1 Cavity expansion model

polar coordinate system ($r$, $\theta$) is defined, and the origin of the coordinate system is located at the initial contact point between indenter and the rock. $r$ and $\theta$ represent the polar radius and the polar angle respectively. The projected contact length between the indenter and the rock is 2$a$. The region with a radius of $a$ beneath the indenter is a hydrostatic core. The outside region of the hydrostatic core is a half-circle plastic zone with the center at the initial contact point. Elastic zone is outside the plastic region and $r_*$ is the radius of the elasto-plastic interface, as shown in Fig. 1.

The radius $r_*$ is normalized to be $\xi_{*=}$ $r_*/a$, and the relationship between $\xi_*$ and $\gamma$ is expressed as follows

$$\gamma = (1+\omega)\xi_*^{(K_d+1)/K_d} - \omega\xi_*^{(K_p-1)/K_p} \tag{1}$$

where, $\gamma$ is determined by the indenter's geometry and the material properties.

$$\gamma = \frac{2\left(K_p+1\right)G\tan\beta}{\pi\sigma_c} \tag{2}$$

$$\mu = \omega K_p/(K_p+K_d) \tag{3}$$

where,

$$K_p = (1+\sin\varphi)/(1-\sin\varphi) \tag{4}$$

$$K_d = (1+\sin\psi)/(1-\sin\psi) \tag{5}$$

$$\omega = \frac{(K_p-1)+(1-2\upsilon)(K_p-1)(K_d-1)}{2K_p} \tag{6}$$

In Eqs. (1)-(6), $\varphi$ is the friction angle, $\psi$ is the dilatancy angle, $\sigma_c$ is the uni-axial compressive strength, $G$ is the shear modulus, $\upsilon$ is the Poisson's ratio, $\beta$ is the inclination angle between the indenter's surface and the rock, $K_p$ is the passive coefficient, and $K_d$ is the dilatancy coefficient.

The indentation pressure on the unit length of the indenter can be estimated from the following equation

based on the interfacial radius of damage zone $\xi_*$.

$$\frac{p}{\sigma_c}=\frac{1}{K_p-1}\left(\frac{2K_p}{K_p+1}\xi_*^{\frac{K_p-1}{K_p}}-1\right) \tag{7}$$

A crack flaw with a length of λ is assumed located at the elasto-plastic interface. With the increase of the indentation depth and the plastic zone, the stress intensity factor $K_I$ at the crack tip may reach the fracture toughness of the rocks $K_{IC}$, which drives the crack propagation radius

$$\frac{d_*}{l}=\frac{2m_1\Lambda^{3/2}}{[\Lambda^{1/2}-m_2(K_p+1)]}\frac{\tan\beta}{\xi_*} \tag{8}$$

$$\Lambda=\lambda/l \tag{9}$$

$$l=(K_{IC}/\sigma_c)^2 \tag{10}$$

where $d_*$ is the critical indentation depth, $m_1$ and $m_2$ are normalized coefficients dependent on the loading types and the geometry of the indenter, $\Lambda$ is the scaled flaw length and $l$ is the material constant.

## 3. Simulation tests on rock indentation

The Ba-Zhong sandstone is taking as an example in this section (Young's modulus $E$ is 9.1 GPa, Poisson's ratio $v$ is 0.14, the compressive strength is 82.4 MPa and the tensile strength is 2.97 MPa), its properties are used to calibrate the micro-properties of the particles, the final selected micro-parameters of the particles are shown in Table 1, and the discrete element simulation model is established which comprises 23 897 balls bond together, the radius is range from 0.075 mm to 0.1125 mm and the rock sample of the size 28 mm×28 mm, the average radius of particles is denoted by $R$, just as Fig.2 shows. The lower surface of the model is constrained by a frictionless rigid wall, the cutter invades the rock with a constant velocity perpendicular to the rock surface. There are two kinds of contact models between particles in PFC, which are contact bond and paralle bond, the parallel bond model is used in this paper. Relative motion at the contact (occurring after the parallel bond has been created) causes a force and a moment generation within the bond material due to the parallel-bond stiffness. This force and moment act on the two-bonded particles, and can be related to maximum normal and shear stresses acting within the bond material at the bond periphery. If either of these maximum stresses exceeds its corresponding bond strength, the parallel bond breaks.

Fig. 3 shows the rock fragmentation process under rock indentation, it illustrates that the region which contact with the indenter will generate elastic strain firstly during the penetration, then the plastic zone forms. With the increasing of penetration depth, the sub-vertical crack initiates along a certain path from the plastic zone and penetrates into the rock mass, and extends to bottom edge of the rock at last. Fig.4 is the indentation force calculated during the indentation in this section. There are several peaks and valleys of indentation force which monitored during the

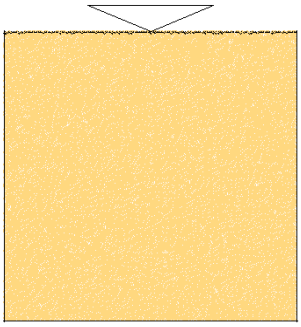

Fig. 2 The discrete element simulation model of rock indentation

Table 1 The micro-properties of the particles

| Particle | | Parallel bond | |
|---|---|---|---|
| $\mu_1$ | 0.5 | $\bar{\lambda}$ | 1.0 |
| $R_{min}$ (*mm*) | 0.075 | pbsn (MPa) | 63±2 |
| $R_{max}/R_{min}$ | 1.5 | pbss (MPa) | 63±2 |
| $E_c$(*GPa*) | 6 | pbm (GPa) | 6 |
| $k_n/k_s$ | 1.2 | pbk | 1.2 |

where, $\mu_1$ represents the contact friction coefficient between two balls, $R_{min}$ represents the radius of minimum ball, $R_{max}/R_{min}$ is the ratio of maximum ball radius to the minimum, $E_c$ is young's modulus of ball, $k_n$ is the contact normal stiffness of balls, $k_s$ is the contact shear stiffness of balls, $\bar{\lambda}$ represents the parallel bound radius factor, pbsn is the parallel normal bond strength, pbss is the parallel shear bond strength, pbm is the young's modulus of parallel bond, pbk is the ratio of parallel bond normal stiffness to shear stiffness.

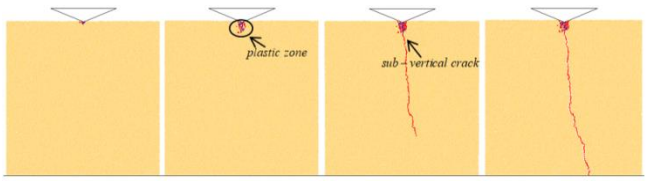


Fig. 3 Rock fragmentation process under rock indentation

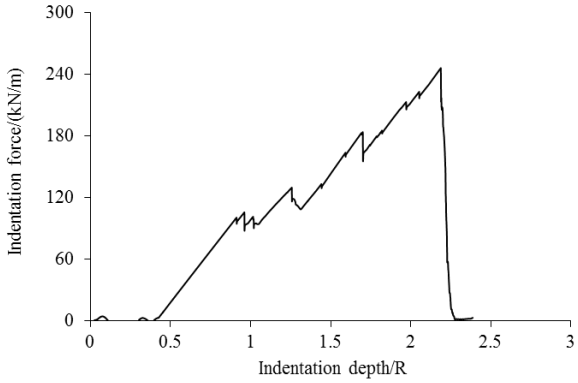


Fig. 4 Indentation force monitored during the indentation

indentation process. The higher force magnitudes imply a higher surface energy status of rock, a sudden decrease of

the cutting force magnitude occurs while sub-vertical crack extend to the bottom edge of rock.

## 4. Experimental tests on rock indentation

The test rig for experiment of rock indentation is shown in Fig. 5, and it is consisted of computer controlled electro-hydraulic servo universal testing machine, acoustic emission equipment, ARAMIS, indenter, rock sample and clamp. Two CCD cameras are placed in front of the rock sample to capture the macroscopic crack propagation. Four acoustic emission probes are installed on the back of the rock sample in counterclockwise direction. The coupling quality of the probe and the rock surface is enhanced through painting vaseline on such surface. Waterproof tape is also used to fix the probes at four specified locations. Four piezoelectric converters are used as the acoustic emission signal sensor, and the acoustic signal can pass through four pre-amplifiers into the system with the fixed threshold value of 34 db. Specially fabricated indenters (four kinds of indenters, including three wedge shapes with angles of 120°, 105° and 90° respectively, and a round shape) are installed at the head of the testing machine, and the rock sample is placed under the indenters. The rock samples are loaded by the testing machine with a speed of 0.0083 mm/s to 5 kN, and then they are unloaded to 3 kN. Such loading process is repeated till the failure of the rock samples. The indentation force is collected through data collection system. In the experimental process, the measured data from three instruments, i.e., computer controlled electro-hydraulic servo universal testing machine, acoustic emission equipment and ARAMIS, are collected simultaneously.

Three kinds of rocks (10 samples of Jian-Yang sandstone, 10 samples of Ba-Zhong sandstone and 15 samples of Sui-Ning granite) are used in the experimental tests. The rocks are cut into samples with size of 230 mm×230 mm×30 mm. The rock samples need to be speckled before the experiments. Firstly, a layer of paint is sprayed uniformly to the sample surface, and then visible speckles are implemented with black coating as shown in Fig. 6.

### *4.1 Mechanism of rock fragmentation in indentation process*

The rock deformation at different moments during the indentation process is shown in Fig. 7. The samples used in the experiments are squared thin-walled plates, and it can be simplified as a two-dimensional body without considering the dimension in the thickness direction. As shown in Fig. 7, elastic strain is firstly generated in the contact region between the rock and the indenter during the penetration process. Sequentially, plastic zone forms. With the increase of the penetration depth, the rock deformation initiates along a path from the plastic zone. Finally, the rock deformation penetrates through the entire structure of the sample.

The damage and degradation of the rocks under indentation can be monitored by using the acoustic emission localization method. The rock will generate tiny fracture


Fig. 5 Rock indentation experiment system

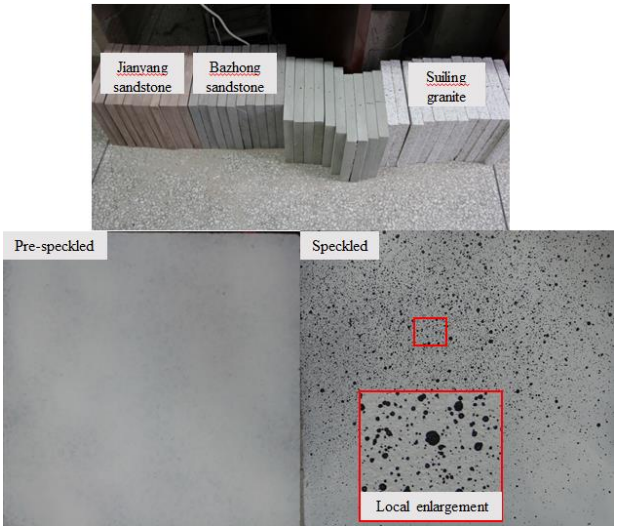


Fig. 6 The speckle processing of rock sample

and release energy, which can be located by acoustic emission testing instrument as seen from Fig. 8. Although the micro-cracks in the rock will not form macro failure, the evolution of the internal damage can be reflected approximately and the direction of the macroscopic crack can be determined roughly from them. Fig. 9 shows the propagation of the macro-crack obtained captured by CCD camera. Comparing with the observations in Fig. 7, it is found that the development of the rock deformation is very similar to the propagation of the macro-crack, which indicates that the generation of the macroscopic crack may be due to the development of the local deformation in the rock. The generated micro-cracks of Ba-Zhong sandstone are shown in Fig. 8, in which Figs. 8(a)-8(d) represent the evolution of the micro-cracks at four different moments. The overall distribution of the micro-cracks is generally consistent with the direction of the macro-crack. During the experiment, the moment of crack initiation is measured based on the results captured from the acoustic emission equipment, ARAMIS and CCD camera.

### *4.2 Evaluation on rock fragmentation efficiency based on plastic energy dissipation ratio*

As mentioned previously, MSE is generally used as an index to evaluate the fragmentation efficiency and drilling efficiency of rocks. The so-called MSE refers to the dissipated energy in breaking a unit volume of rocks.

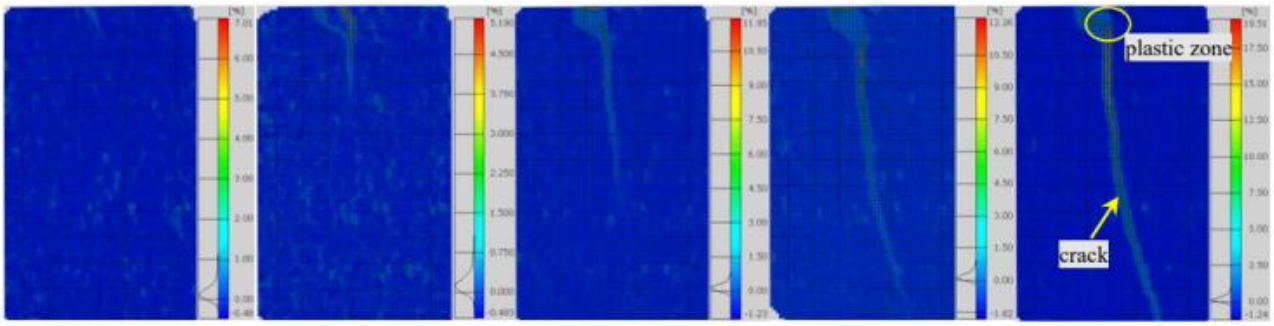


Fig. 7 The deformation of Ba-Zhong sandstone at different moments

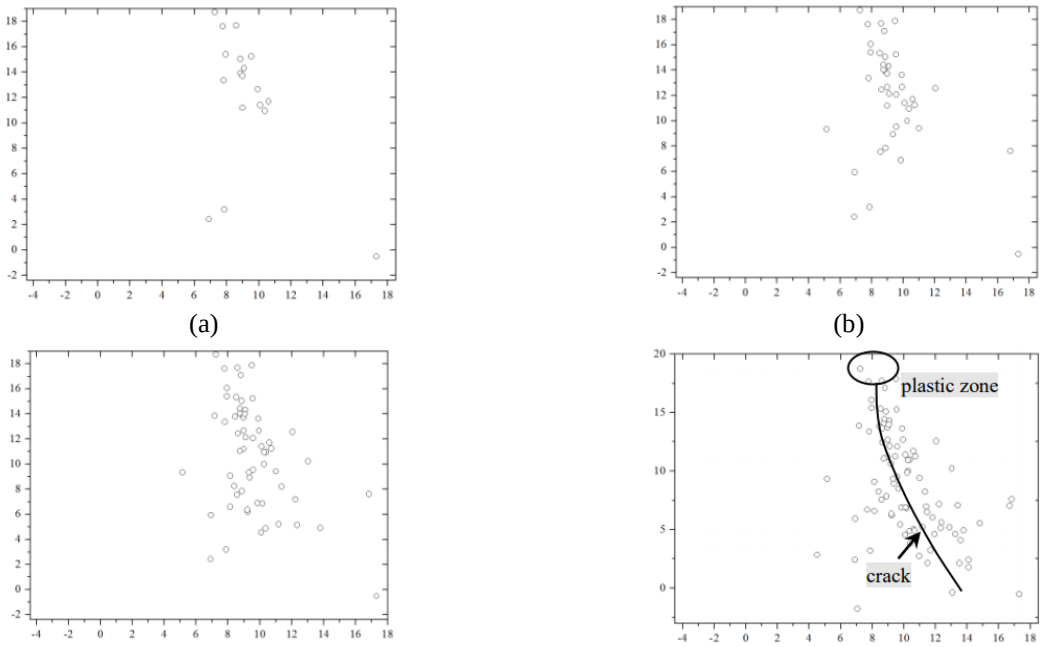


Fig. 8 The damage and degradation of Ba-Zhong sandstone at different moments

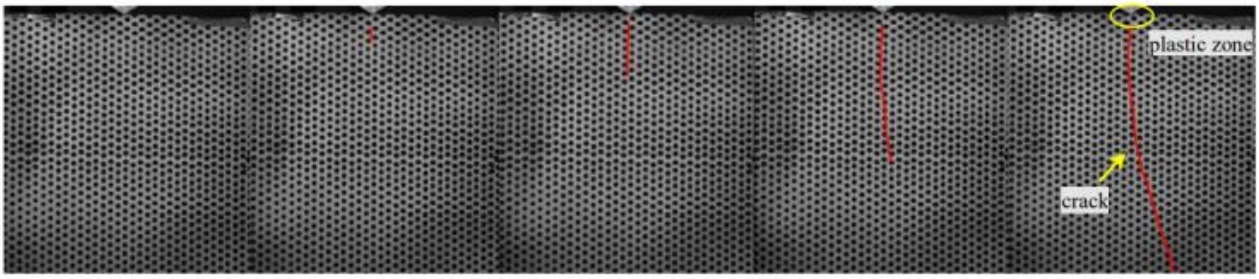


Fig. 9 Expansion of macro crack obtained by CCD camera

However, such dissipated energy is not divided into different parts any more. This study presented a new parameter named plastic energy dissipation ratio to represent the amount of the dissipated plastic energy in the rock fragmentation. Since the plastic deformation is inevitable during the indentation process, the energy dissipated by plastic deformation cannot cause the energy dissipated by brittle fracture can result in the crack initiation, propagation and coalescence, the greater the plastic energy dissipation ratio the less efficient the rock generation of fractures and rock chips, instead, the fragmentation, this quantity can be used to analyze the fragmentation efficiency of rocks.

The failure modes of rocks can be divided into two stages according to the indentation process: one is due to plastic deformation of the rocks with the indentation process, and the other one is initiation and propagation of crack in the plastic zone (basically, no plastic deformation is accumulated in this stage). In the first stage, the work done by the indenter to the rocks is only transferred to the energy

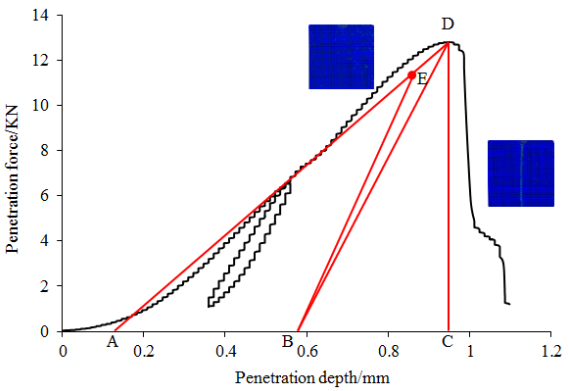


(a) Wedge-shaped 90° indenter

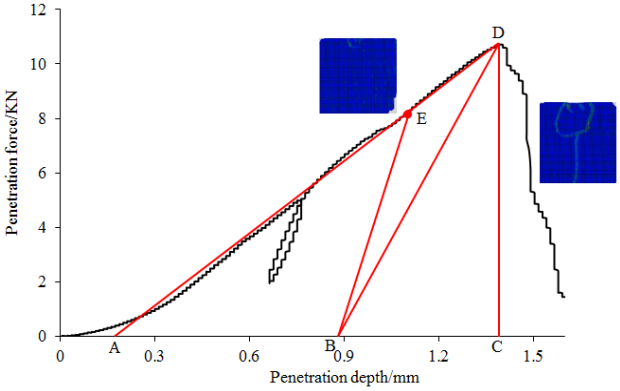


(b) Wedge-shaped 105° indenter

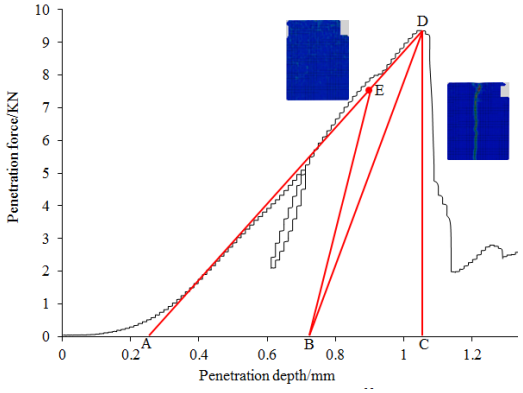


(c) Wedge-shaped 120° indenter

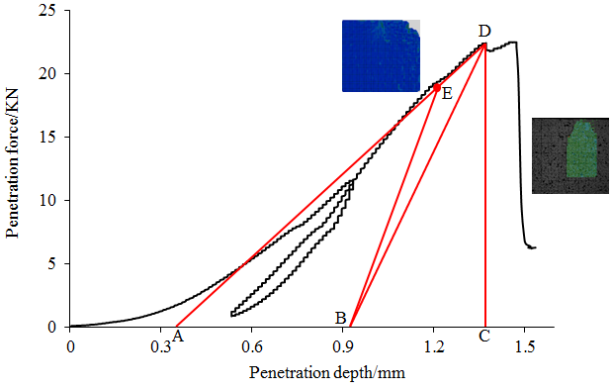


(d) Roundness-shaped 120° indenter

Fig. 10 The load-penetration history and linear unloading simulation of Jian-Yang sandstone

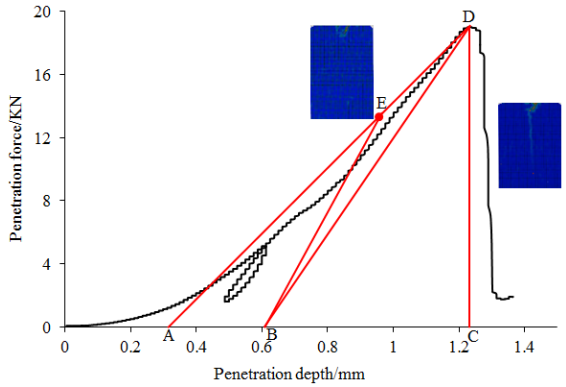


(a) Wedge-shaped 90° indenter

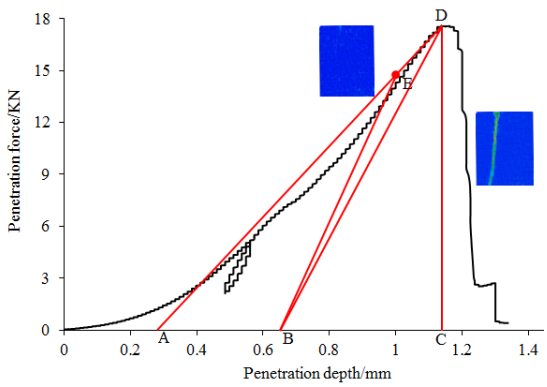


(b) Wedge-shaped 105° indenter

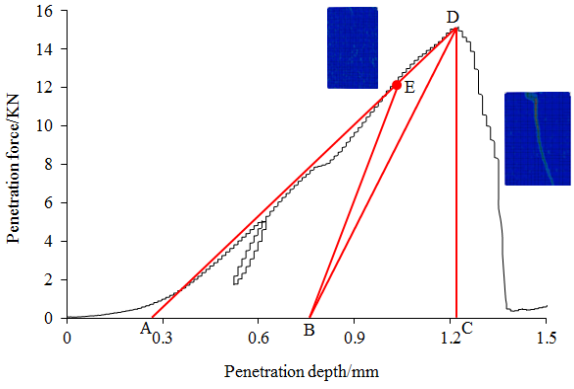


(c) Wedge-shaped 120° indenter

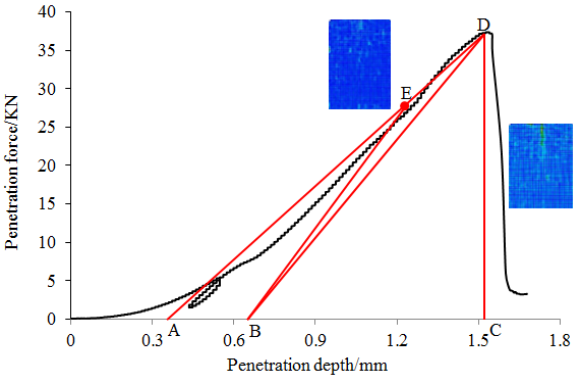


(d) Roundness-shaped 120° indenter

Fig. 11 The load-penetration history and linear unloading simulation of Ba-Zhong sandstone

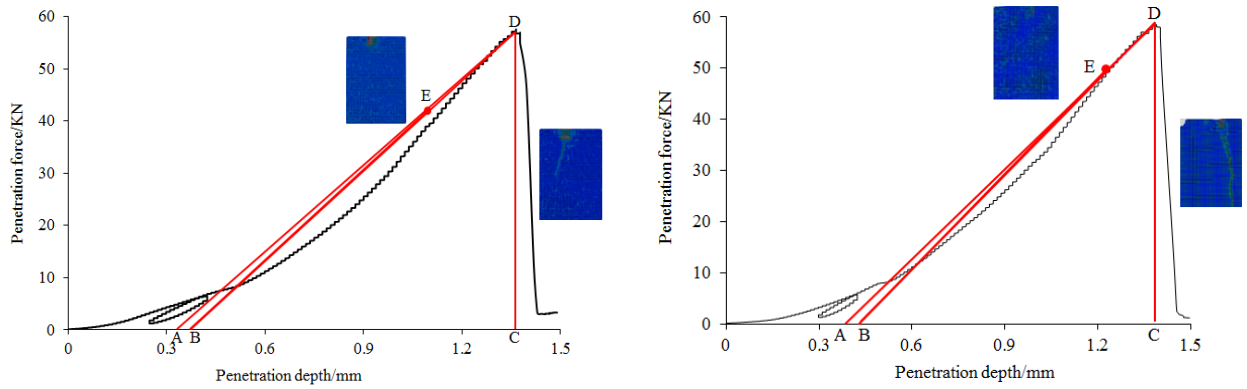


(a) Wedge-shaped 105° indenter (b) Wedge-shaped 120° indenter

Fig.12 The load-penetration history and linear unloading simulation of Sui-Ning granite

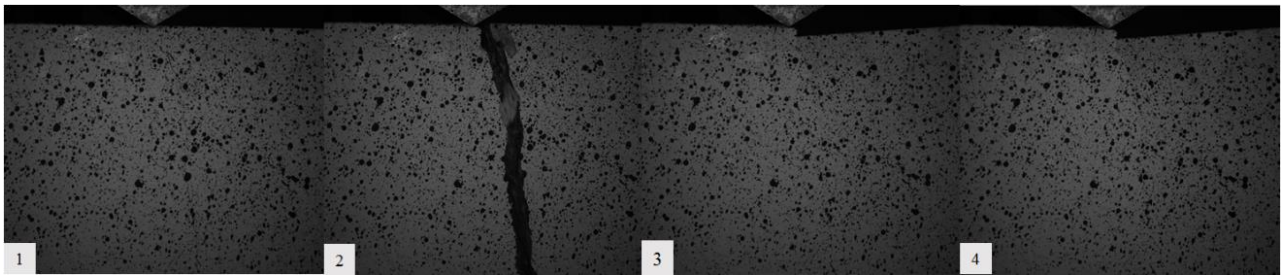


Fig.13 The breaking process of Sui-Ning granite

dissipated by the elastic and plastic deformations of the rocks, and it is expressed as follows

$$E_T = E_e + E_p \tag{11}$$

$$\frac{E_p}{E_T} = 1 - \frac{E_e}{E_T} = 1 - \frac{(K_p - 1)}{\gamma[2K_p \xi_*^{(K_p-1)/K_P} - K_p - 1]} \tag{12}$$

where, $E_T$ is the total dissipated energy, $E_e$ is the elastic energy, $E_p$ is the plastic energy.

In the second stage after the crack initiation, the elastic energy is released to cause the form of new surfaces in the rocks due to crack propagation. At this moment, the work done by the indenter is mainly consumed in the elastic and plastic deformations of the rocks as well as in the brittle breaking. The total dissipated energy is expressed as follows

$$E_T = E_e + E_p + E_f \tag{13}$$

where, $E_f$ is the dissipated energy on the form of the crack surface.

Analyses on the energy dissipation of the three parts in Eq. (16) are significant for the fragmentation mechanism of the rocks during the indentation process. Figs. 10-12 illustrate relationship of the penetration force and the penetration depth of three kinds of rock samples under wedge-shaped indentation. Before the crack initiation, the work done by the indenter to the rocks is dissipated to the elastic and plastic deformations of the rocks. Point *E* in the figures refers to the crack initiation, and it is determined from the measured strain and the observation from the CCD camera. The slope line *BE* is parallel to the unloading line.At point *E*, brittle breaking of rocks is observed. The work of the indenter to the rocks is used to generate new surface due to the form of new cracks. Plastic energy dissipated in this process is not changed. The area of ΔACD in the figures refers to the work done by the indenter to the rocks. From elasticity and plasticity theory, the area of ΔABE is the dissipated plastic energy of the rocks, and the areas of ΔBCD and ΔBDE are the dissipated elastic energy and the dissipated energy for brittle breaking of rocks respectively. From simple calculations in Fig. 10(a), the areas of ΔABE, ΔBCD and ΔBDE are 2.69 kN.mm, 2.43 kN.mm and 0.13 kN.mm respectively. It is then found that the ratio of the elastic energy, plastic energy and the brittle breaking energy dissipated in the indentation process is $E_e$:$E_p$:$E_f$ =18.69: 20.69:1. The ratio of the dissipated plastic energy to the total dissipated energy is 1:1.95. Similarly, the ratios of the elastic energy, plastic energy and the brittle breaking energy dissipated in the indentation process in Figs. 10(b)-10(d) are 3.21:3.47:1, 3.95:4.46:1 and 5.73:6.55:1 respectively, and the ratios of the dissipated plastic energy to the total dissipated energy are 1:2.21, 1:2.11 and 1:2.02 respectively. Through the comparison of the dissipated plastic energy ratio in Figs. 10(a)-10(d), it is concluded that the indenter with a wedged angle of 105° has the minimum value of the dissipated plastic energy ratio, and its rock fragmentation efficiency is highest. On the contrary, the indenter with a wedged angle of 90° has the maximum value of dissipated plastic energy ratio, and its rock fragmentation efficiency is lowest.

Through similar analyses and calculations, the ratios of the elastic energy, the plastic energy and the brittle breaking

energy of the rocks dissipated in the indentation process are 6.58:2.13:1, 6.09:3.91:1, 3.67:2.92:1 and 10.29:2.6:1 respectively in Figs. 11(a)-11(d). The ratios of the dissipated plastic energy to the total dissipated energy are 1:4.56, 1:2.81, 1:2.6 and 1:5.35 respectively. It is found from the comparison that the round indenter dissipated least plastic energy, and its rock fragmentation efficiency is highest. However, the critical penetration force of the round indenter is also large, and the total energy dissipated in the indentation process becomes more, which has harmful effect to the life of the drill bit. Therefore, this kind of indenter is not recommended. The wedge-shape indenter with a wedged angle of $120^o$ dissipates most plastic energy, and its rock fragmentation efficiency is lowest.

The relationship of the penetration force and the penetration depth for Sui-Ning granite is shown in Fig. 12. It is found that most of the work done by the indenter is transferred to elastic energy of the rocks, and the dissipated energy of the rocks for plastic deformation and brittle breaking is very little, which is coincident with experimental observations. When the samples are loaded to 5 kN and then unloaded, it is observed that the unloading curve can return to the origin, which implies that only elastic deformation exists and no plastic deformation is accumulated in this loading stage. With continuous loading from the indenter, noise can be heard from the rock, and such may be produced due to the dislocation of the internal crystals in the rocks. With further indentation, the rock samples are split into two halves suddenly without any warning symbol. Fig. 13 shows four moments of the sample before and after fracture, and the time interval for any two adjacent pictures is 0.17 s. Crack initiates and propagates in the first picture. The rock sample is split to two halves by a crack as shown in the second picture, and the distance between the crack surfaces is much bigger. It is found that most work done by the indenter is transferred to elastic energy for the rocks with high hardness and brittleness. Little energy is dissipated in the plastic deformation and brittle breaking of the rocks. The elastic energy is then mainly transferred to the kinetic energy of the rock fragment.

In overall, it is found from Figs. 10-12 that the plastic energy dissipation ratio becomes lower in the rock fragmentation process for the rocks with high hardness and brittleness, and vice versa. For example, the ratio of the dissipated plastic energy to the total dissipated energy of Jian-Yang sandstone is 1:2.11 when a wedge-shape indenter with a wedged angle of $120^o$ is used.

For the Ba-Zhang sandstone, such ratio is 1:2.6, while the dissipated plastic energy of the granite can be ignored.

## 5. Conclusions

The plastic energy dissipation ratio is proposed as an index to identify the rock fragmentation efficiency in this paper. Using this method, the fragmentation efficiency of rocks with different values of hardness is analyzed. In addition, the rock failure mechanism in the indentation process is also analyzed through theoretical, numerical simulation and experimental analysis. The results of this research revealed the following findings.

• The formation of the plastic zone beneath the indenter acts as a prelude to crack initiation and propagation. As the indenter penetrates into rock, the sub-vertical crack is generated from the plastic zone and extended to bottom edge of the rock at last;

• It is found that the rock fragmentation efficiency is higher when the plastic energy dissipation ratio is lower for a given kind of rock. The experiment on Jian-Yang sandstone indicates that the rock fragmentation efficiency is the highest for the wedge-shape indenter with a wedged angle of $105^o$ while such efficiency becomes lowest when the indenter with a wedged of 90° is used. For the Ba-Zhong sandstone, the round indenter has the highest rock fragmentation efficiency and the wedge-shape indenter with a wedged angle of $120^o$ has the lowest efficiency;

• The plastic energy dissipation ratio is lowest for the rocks with high hardness and brittleness. For the rocks with low hardness (sandstone), most of the work done by the indenter to the rocks is transferred to elastic and plastic energy of the rocks. For the rocks with high hardness and brittleness, most of the work is transferred to elastic energy of the rocks, and the dissipated energy for plastic deformation and brittle breaking of the rocks is little. Such elastic energy is mainly transferred to kinetic energy of the rock fragments.

## Acknowledgements

This study is supported by the National Natural Science Foundation of China (Grant No.51674214), International Cooperation Project of Sichuan Science and Technology Plan (2016HH0008), Youth Science and Technology Innovation Research Team of Sichuan Province (2017TD0014). Such supports are greatly appreciated by the authors.

## References

Alehossein, H., Detournay, E. and Huang, H. (2000), "An analytical model for the indentation of rocks by blunt tools", *Rock Mech. Rock Eng.*, **33**(4), 267-284.

Augustine, C.R. (2009), "Hydrothermal spallation drilling and advanced energy conversion technologies for engineered geothermal systems", Ph.D. Dissertation, Massachusetts Institute of Technology, Massachusetts, U.S.A.

Carpinteri, A. and Invernizzi, S. (2005), "Numerical analysis of the cutting interaction between indenters acting on disordered materials", *J. Fract.*, **131**(2), 143-154.

Carpinteri, A., Chiaia, B. and Invernizzi, S. (2004), "Numerical analysis of indentation fracture in quasi-brittle materials", *Eng. Fract. Mech.*, **71**(4), 567-577.

Chen, L.H. and Labuz, J.F. (2006), "Indentation of rock by wedge-shaped tools", *J. Rock Mech. Min. Sci.*, **43**(7), 1023-1033.

Chen, L.S., Huang, G.Z. and Chen, Y.C. (2009), "Acoustic emission evolution in indentation fracture of rocks under different lateral pressure free boundaries", *Chin. J. Rock Mech. Eng.*, **28**(12), 2411-2420 (in Chinese).

Chen, S., Grosz, G., Anderle, S., Arfele, R. and Xun, K. (2015), "The role of rock-chip removals and cutting-area shapes in polycrystalline-diamond-compact-bit design optimization", *SPE*

*Drill. Completion*, **30**(4), 334-347.
Detournay, E., Fairhurst, C. and Labuz, J.F. (1995), "A model of tensile failure initiation under an indentor", *Proceedings of the 2nd International Conference on Mechanics of Jointed and Faulted Rock (MJFR-S)*, Vienna, Austria, April.
Gillis, P.J., Gillis, I.G. and Knull, C.J. (2004), *Rotational Impact Drill Assembly*, U.S. Patent 6,742,609, U.S. Patent and Trademark Office, Washington, D.C., U.S.A.
Han, G. and Bruno, M.S. (2006), "Percussion drilling: From lab tests to dynamic modeling", *Proceedings of the International Oil & Gas Conference and Exhibition in China*, Beijing, China, December.
Huang, H. (1999), "Discrete element modeling of rock-tool interaction", Ph.D. Dissertation, University of Minnesota, Minnesota, U.S.A.
Huang, H. and Detournay, E. (2013), "Discrete element modeling of tool-rock interaction II: Rock indentation", *J. Numer. Anal. Meth. Geomech.*, **37**(13), 1930-1947.
Huang, H., Damjanac, B. and Detournay, E. (1998), "Normal wedge indentation in rocks with lateral confinement", *Rock Mech. Rock Eng.*, **31**(2), 81-94.
Johnson, K.L. (1970), "The correlation of indentation experiments", *J. Mech. Phys. Solids*, **18**(2), 115-126.
Johnson, K.L. (1987), *Contact Mechanics*, Cambridge University Press.
Kolle, J.J. (2000), "Coiled-tubing drilling with supercritical carbon dioxide", *Proceedings of the SPE/CIM International Conference on Horizontal Well Technology*, Calgary, Canada, November.
Kuang, Y.C., Zhu, Z.P. and Jiang, H.J. (2012), "The Experimental study and numerical simulation of single particle impacting rock", *Acta Petrolei Sinica*, **33**(6), 1059-1063 (in Chinese).
Lawn, B. and Wilshaw, R. (1975), "Indentation fracture: principles and applications", *J. Mater. Sci.*, **10**(6), 1049-1081.
Lawn, B.R. and Evans, A.G. (1977), "A model for crack initiation in elastic/plastic indentation fields", *J. Mater. Sci.*, **12**(11), 2195-2199.
Lawn, B.R. and Swain, M.V. (1975), "Microfracture beneath point indentations in brittle solids", *J. Mater. Sci.*, **10**(1), 113-122.
Liu, H.Y., Kou, S.Q., Lindqvist, P.A. and Tang, C.A. (2002), "Numerical simulation of the rock fragmentation process induced by indenters", *J. Rock Mech. Min. Sci.*, **39**(4), 491-505.
Marshall, D.B. (1984), "Measurement of dynamic hardness by controlled sharp projectile impact effects in elastic/plastic indentation", *Amer. Ceram. Soc.*, **67**(1), 580-585.
Martinez, I.M.R., Fontoura, S., Inoue, N., Carrapatoso, C.M., Lourenço, A. and Curry, D. (2013), "Simulation of single cutter experiments in evaporites through finite element method", *Proceedings of the SPE/IADC Drilling Conference and Exhibition*, Amsterdam, The Netherlands, March.
Melamed, Y., Kiselev, A., Gelfgat, M., Dreesen, D. and Blacic, J. (2000), "Hydraulic hammer drilling technology: Developments and capabilities", *J. Energy Resour. Technol.*, **122**(1), 1-7.
Mendoza, R.J.A. (2013), "Considerations for discrete element modeling of rock cutting", Ph.D. Dissertation, University of Pittsburgh, Pittsburg, Pennsylvania, U.S.A.
Mo, Z.Z., Li, H.B., Zhou, Q.C., Zou, F., Zhu, X.M., Wang, C.B. and Hao, Y.F. (2012), "Experimental study of microscopic deterioration under wedge cutter", *Rock Soil Mech.*, **33**(5), 1333-1340 (in Chinese).
Ni, H.J., Wang, R.H. and Ge, H.K. (2004), "Numerical simulation on rock fragmentation under high pressure water jet", *Chin. J. Rock Mech. Eng.*, **23**(4), 550-554 (in Chinese).
Oothoudt, T. (1999), "The benefits of sonic core drilling to the mining industry", *Proceedings of the 6th International Conference on Tailings and Mine Waste '99*, Fort Collins, Colorado, U.S.A., January.
Paluszny, A., Zimmerman, R.W., Potjewyd, J. and Jarvis, B. (2014), "Finite element-based numerical modeling of fracture propagation due to the plunge of a spherical indenter", *Proceedings of the 48th US Rock Mechanics/Geomechanics Symposium*, Minneapolis, Minnesota, U.S.A., June.
Rajabov, V., Miska, S.Z., Mortimer, L., Yu, M. and Ozbayoglu, M.E. (2012), "The effects of back rake and side rake angles on mechanical specific energy of single PDC cutters with selected rocks at varying depth of cuts and confining pressures", *Proceedings of the IADC/SPE Drilling Conference and Exhibition*, San Diego, California, U.S.A., March.
Ren, J.H., Xu, Y.J., Zhao, J., Zhao, X.L. and Zhang, M. (2011), "Numerical simulation analysis of particle impacting breaking rock", *Chin. J. High Pressure Phys.*, **26**(1), 89-94 (in Chinese).
Sherrit, S., Bao, X., Chang, Z., Dolgin, B. P., Bar-Cohen, Y., Pal, D., Kroh, J. and Peterson, T. (2000), "Modeling of the ultrasonic/sonic driller/corer: USDC", *Proceedings of the 2000 IEEE Ultrasonics Symposium*, San Juan, Puerto Rico, October.
Sinha, P. and Gour, A. (2006), "Laser drilling research and application: An update", *Proceedings of the SPE/IADC Indian Drilling Technology Conference and Exhibition*, Mumbai, India, October.
Souissi, S., Hamdi, E. and Sellami, H. (2015), "Microstructure effect on hard rock damage and fracture during indentation process", *Geotech. Geol. Eng.*, **33**(6),1539-1550.
Swain, M.V. and Hagan, J.T. (1976), "Indentation plasticity and the ensuing fracture of glass", *J. Phys. D Appl. Phys.*, **9**(15), 2201.
Tan, X.C., Kou, S.Q. and Lindqvist, P.A. (1998), "Application of the DDM and fracture mechanics model on the simulation of rock breakage by mechanical tools", *Eng. Geol.*, **49**(3), 277-284.
Tao, X.H., Zhang, J.L. and Zeng, Y.J. (1998), "Study and application of rotary percussion drilling technology", *Oil Drill. Prod. Technol.*, **20**(2), 27-30 (in Chinese).
Teale, R. (1965), "The concept of specific energy in rock drilling", *J. Rock Mech. Min. Sci. Geomech. Abstr.*, **2**(1), 57-73.
Wang, S.Y., Sloan, S.W., Liu, H.Y. and Tang, C.A. (2011), "Numerical simulation of the rock fragmentation process induced by two drill bits subjected to static and dynamic (impact) loading", *Rock Mech. Rock Eng.*, **44**(3), 317-332.
Wilkinson, M.A. and Tester, J.W. (1993), "Experimental measurement of surface temperatures during flame-jet induced thermal spallation", *Rock Mech. Rock Eng.*, **26**(1), 29-62.
Xu, Y.J. (2004), "Basic research on the theory and application of super high pressure water jet", Ph.D. Dissertation, Southwest Petroleum University, Chengdu, China
Xu, Z., Reed, C.B., Leong, K.H., Parker, R.A. and Graves, R.M. (2003), "Application of high powered lasers to perforated completions", *Proceedings of the International Congress on Applications of Laser & Electro-Optics*, Jacksonville, Florida, U.S.A.
Yin, L.J., Gong, Q.M., Ma, H.S., Zhao, J. and Zhao, X.B. (2014), "Use of indentation tests to study the influence of confining stress on rock fragmentation by a TBM cutter", *J. Rock Mech. Min. Sci.*, **72**, 261-276.
Zhang, H. and Song, H. (2013b), "Experimental investigation on deformation and failure of rock under cyclic indentation", *Proceedings of the International Conference on Fracture*, Beijing, China, June.
Zhang, H., Huang, G., Song, H. and Kang, Y. (2012), "Experimental investigation of deformation and failure mechanisms in rock under indentation by digital image correlation", *Eng. Fract. Mech.*, **96**, 667-675.
Zhang, H., Song, H., Kang, Y., Huang, G. and Qu, C. (2013a), "Experimental analysis on deformation evolution and crack propagation of rock under cyclic indentation", *Rock Mech. Rock Eng.*, **46**(5), 1053-1059.

Zhou, Y. and Lin, J.S. (2014), "Modeling the ductile-brittle failure mode transition in rock cutting", *Eng. Fract. Mech.*, **127**, 135-147.

Zhou, Y., Zhang, W., Gamwo, I.K., Lin, J.S., Eastman, H., Whipple, G. and Gill, M. (2012), "Mechanical specific energy versus depth of cut", *Proceedings of the 46th US Rock Mechanics/Geomechanics Symposium*, Chicago, Illinois. U.S.A., June.

Zhu, X., Liu, W. and He, X. (2017), "The investigation of rock indentation simulation based on discrete element method", *KSCE J. Civ. Eng.*, **21**(4), 1201-1212.

Zhu, X., Tang, L. and Tong, H. (2014), "Effects of high-frequency torsional impacts on rock drilling", *Rock Mech. Rock Eng.*, **47**(4), 1345-1354.

*CC*